Heterogeneous & Homogeneous & Bio- & Nano-
CHEMCATCHEM
CATALYSIS

Accepted Article

Title: Vapor Phase Hydrogenolysis of Furanics Utilizing Reduced Cobalt Mixed Metal Oxide Catalysts

Authors: Taylor P Sulmonetti, Bo Hu, Zachary P Ifkovits, Sungsik Lee, Pradeep K. Agrawal, and Christopher W Jones

To be cited as: *ChemCatChem* 10.1002/cctc.201700228

Link to VoR: http://dx.doi.org/10.1002/cctc.201700228

A Journal of
ChemPubSoc Europe

WILEY-VCH

www.chemcatchem.org

10.1002/cctc.201700228

WILEY-VCH

FULL PAPER

Vapor Phase Hydrogenolysis of Furanics Utilizing Reduced Cobalt Mixed Metal Oxide Catalysts

Taylor P. Sulmonetti,[a] Bo Hu,[a] Zachary Ifkovits,[a] Sungsik Lee,[b] Pradeep K. Agrawal[a] and Christopher W. Jones[a*]

Abstract: Vapor phase hydrogenolysis of both furfuryl alcohol and furfural were investigated over reduced Co based mixed metal oxides derived from the calcination of a layered double hydroxide precursor. Although a reduced cobalt aluminate sample displays promising selectivity towards 2-methylfuran (2-MF) production, the addition of an Fe dopant into the oxide matrix significantly enhances the activity and selectivity per gram of catalyst. Approximately 82% 2-MF yield is achieved at high conversion when furfuryl alcohol is fed into the reactor at 180 °C over the reduced 3Co-0.25Fe-0.75Al catalyst. Based on structural characterization studies including TPR, XPS, and *in-situ* XAS it is suggested that Fe facilitates the reduction of Co, allowing for formation of more metallic species. Overall, this study demonstrates that non-precious metal catalysts offer promise for the selective conversion of a key biomass oxygenate to a proposed fuel additive.

Introduction

Second generation lignocellulosic biomass, the inedible fraction of biomass, is a target for conversion into chemicals and fuel additives because of its perceived likelihood to not interrupt food supplies.[1,2] Lignocellulose can be broken down into various sugars that can be further processed through dehydration to create furanic compounds. Furfural (FUR) and furfuryl alcohol (FA) are major platform chemicals in biomass processing that can be catalytically converted into valuable products such as tetrahydrofurfuryl alcohol (THFA), 2-methylfuran (2-MF), 1,2-pentanediol (1,2-PD), and 1,5-pentanediol (1,5-PD), among others.[3] Through the hydrogenolysis of FA, 2-MF is produced, which is a valuable fuel additive. With a research octane number of 131 and low water solubility, 2-MF is an attractive replacement for bio-ethanol as a fuel additive.[4] Therefore, recent research has focused on catalytically converting FUR and/or FA selectively towards 2-MF.

Industrially, Cu-Cr catalysts have shown versatility in FUR conversion, and at certain conditions, these catalysts give high yields towards 2-MF.[5] However, due to environmental concerns associated with Cr, development of alternative catalysts is worthwhile. Many monometallic catalysts, typically supported on silica, have been investigated for hydrogenation of furanic compounds. However, these typically suffer from poor selectivities towards 2-MF.[6,7] Improvements in selectivity for catalytic conversion of furanics has often been achieved by the incorporation of multiple metals to form bimetallic or bifunctional catalysts. In this work, the term bimetallic catalyst will refer to a catalyst that contains two fully reduced metals forming an alloy, while the term bifunctional catalyst will refer to catalysts that combine a metallic species and metal oxide species, which may form acidic or basic sites.[8] In regards to 2-MF production, prior work involving Ni-Fe/SiO_2 has been conducted to investigate the enhancement in selectivity that occurs when a secondary metal is added.[9] Through DFT and kinetic studies, it was suggested that the oxophilicity of Fe facilitated the adsorption of FA through a η^2-(C,O) surface species, which drove the reaction towards hydrogenolysis of the C=O bond.[9,10] Additionally, very recent studies conducted with Cu-Fe supported on carbon and silica also demonstrated a synergistic effect between the more oxophilic Fe species and the more reduced Cu species for hydrogenation and hydrogenolysis of FUR.[11,12] Temperature programmed desorption (TPD) and high resolution electron energy loss spectroscopy (HREELS) under ultra-high vacuum conducted on Pt-Zn catalysts suggested a similar mechanism, where Zn acted as the oxophilic metal and allowed for a tilted adsorption mode to be more prevalent on the catalyst surface.[13] Other vapor phase reactions have been conducted with multiple metal systems including Cu-Zn-Al and Cu-Zn-Al-Ca-Na.[14,15] Lastly, Mo_2C catalysts have been shown to be selective towards 2-MF due to the creation of two active sites (bifunctional), a "metal-like site" and a carbidic oxycarbidic, or oxide site; however, the type of secondary site remains unknown based on the evidence presented to date.[16]

Many investigations involving liquid phase reactions, both flow and batch, for the hydrogenolysis of furanics including FUR to 2-MF and hydroxymethylfurfural (HMF) to 2,5-dimethylfuran (DMF) have been performed, mainly involving multiple metal catalyst systems. In regards to HMF to DMF, Ni/Co_3O_4, Ru/Co_3O_4, Ni-W_2C/C, Cu-Ru/C, Pt-Co/C, Cu-Co/C and Cu-ZnO have been investigated, and in regards to FUR to 2-MF, Ru-RuO_2/C, Cu-Co/Al_2O_3, and Pd/TiO_2 have been utilized.[4,17–25] Unfortunately, many of these reactions require high H_2 pressures, have low product throughput, and/or use precious metals, which makes vapor phase flow reactions with non-precious metals a potentially attractive alternative. Consequently, in this work, we sought to create a non-precious, multi-metal system that would be selective towards hydrogenolysis of the C-O bond of FA in vapor phase flow reactions.

A previous study involving Co-Al mixed metal oxides derived from layered double hydroxides (LDH) displayed elevated selectivities

[a] T. P. Sulmonetti, Dr. B. Hu, Z. Ifkovitis, Prof. P. K. Agrawal, Prof. C. W. Jones
School of Chemical & Biomolecular Engineering
Georgia Institute of Technology
311 Ferst Dr., Atlanta, GA 30332, USA
cjones@chbe.gatech.edu
Fax: (+1) 404-894-2866
[b] S. Lee
Advanced Photon Source
Argonne National Laboratory
Lemont, IL 60439, USA

Supporting information for this article is given via a link at the end of the document.

towards 2-MF in the vapor phase hydrogenation of FUR at 155 °C.[26] Use of LDH materials as precursors to synthesize mixed metal oxides is a well-known approach to create well-dispersed and relatively high porosity materials.[27] The LDH material allows for high interaction between the various metals in the matrix, and can lead to smaller metal domains upon reduction. To this end, Co was chosen as the base metal in the catalyst family explored here, while various Fe amounts were added into the matrix to tailor the activity and selectivity. Reduction with hydrogen allowed for the creation of active metallic species, and through temperature-programmed reduction (TPR), X-ray absorption spectroscopy (XAS), and X-ray photoelectron spectroscopy (XPS) it is shown that the incorporation of Fe facilities reduction at lower temperatures, which in turn enhances both selectivity and activity towards 2-MF.

Results and Discussion

Our main interest in LDH based materials is that the synthesis procedure allows for versatility in metal additions while maintaining similar physical properties. After calcination of these materials, the intercalated anions are removed, leaving a porous mixed metal oxide with high dispersion of metal oxide species. This high dispersion suggests intimate contact of various metal species, which could improve activity or selectivity of the catalyst. To that end, Co was chosen as the base metal in the system due to the unique selectivity properties previously determined in FUR reduction.[26] Along with Co, small amounts of Fe were added into the mixed metal oxide matrix to tune the activity and selectivity towards 2-MF. In Table 1, the physical properties are summarized for various Co/Fe ratio.

The porosity of the post calcined LDH materials is displayed in Table 1, which shows that the BET surface area for all materials was within a narrow range (105 m^2/g-150 m^2/g), while the pore volumes were approximately 0.30 cm^3/g. ICP analyses were in fairly good agreement with the targeted molar ratios, with slightly lower Co amounts than anticipated. For simplicity throughout the manuscript, the catalysts were labeled with their target molar ratios.

Table 1: Physical properties of multiple Co based mixed metal oxides.

Catalyst	Elemental analysis (Co:Fe:Al)	BET Surface Area (m^2/g)	Pore Volume (cm^3/g)	Average Pore Diameter (nm)
3Co-Al	2.94:0:1.0	129	0.35	11.0
3Co-0.25Fe-0.75Al	2.83:0.25:0.75	150	0.32	8.6
3Co-0.5Fe-0.5Al	2.83:0.50:0.50	133	0.30	8.7
3Co-0.75Fe-0.25Al	2.92:0.74:0.26	115	0.31	10.4
3Co-Fe	2.93:1.0:0	107	0.33	12.1

After calcination at 400 °C, most LDH materials lose their layered structure to create a more homogeneous mixed metal oxide (MMO). Through XAS and XPS analysis, it was determined that the majority of the crystalline species present after calcination were Co_3O_4, Fe_2O_3, and Al_2O_3, and there was no indication of CoO, FeO, or significant metal aluminate species. The XRD patterns of the uncalcined material are shown in Figure S2, which display prominent (003) and (006) peaks. These peaks represent the layered hydroxides with intercalating CO_3^{-2} and H_2O to balance framework charge. The XRD patterns post calcination

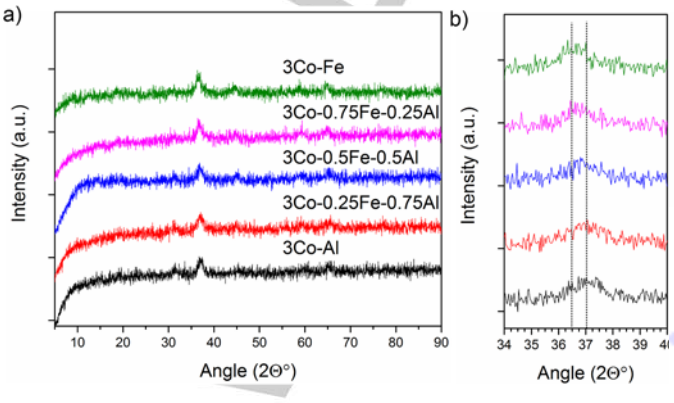

Figure 1: a) XRD patterns of Co-xFe-yAl catalysts after calcination at 400 °C; b) Enlarged section of major Bragg peak between 35-40°.

demonstrated that a non-crystalline structure was created, as evidenced by the lack of sharp peaks associated with the oxides present in Figure 1a. One broad peak is distinguishable between 35-40°, which correlates with the Co_3O_4 (311) peak at 37.0°. Additionally, when that section is enlarged in Figure 1b, there was a small yet noticeable shift to lower Bragg angles with the increased addition of Fe. The poor crystallinity along with the shift in the Co_3O_4 (311) peak towards the Fe_2O_3 (311) peak at 35.0°, along with no visible Al_2O_3 peaks, might suggest good dispersion of the oxide species, potentially forming a solid solution similar to Ni-Co-Al and Ni-Mg-Al mixed metal oxides reported in prior literature.[26–28]

The reduction profile of each catalyst was investigated through TPR to gather information about the catalyst under an H_2 atmosphere with varying temperature. Figure 2 shows the reduction profile of each catalyst in 10% H_2/Ar using a 5 °C/min ramp rate. All five profiles demonstrate a two-step reduction, one at a low temperature between 200 °C- 300 °C and one at a high temperature between 400 °C - 750 °C. The low temperature peaks may refer to Co_3O_4 and Fe_2O_3 phases reducing to CoO and Fe_3O_4/FeO, while the broad, high temperature peak is associated with the reduction of cobalt and iron oxide species to metallic Co and Fe.[28,29] As expected, the addition of Fe slightly shifted the peak reduction temperature to lower temperatures since the reduction potential of Fe oxide was much greater than Al_2O_3. Without any Al_2O_3, the TPR profile became much sharper, and the H_2 uptake began to significantly decline around 500 °C. This indicates that the Al_2O_3 acts as a stabilizer, even at 6.6

wt% in the matrix, since it was unable to reduce under these conditions, and may help prevent complete aggregation of metallic species.

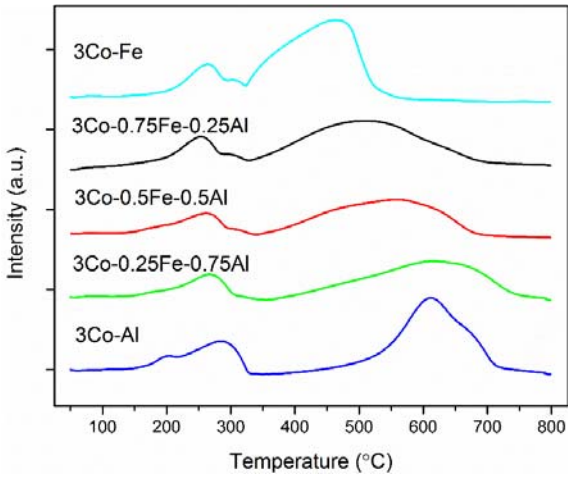

Figure 2: TPR profile of each Co-xFe-yAl catalyst in a 10% H_2 (balance Ar) atmosphere with a 5 °C/min ramp rate.

Initial reaction studies with FA as the substrate were conducted at a common weight hourly space velocity (WHSV) to screen the various catalysts synthesized. Further studies were conducted on the 3Co-0.25Fe-0.75Al catalyst due to the observed high activity of this sample during the initial screening. When comparing the catalysts at similar WHSV, noticeable differences in conversion were observed.

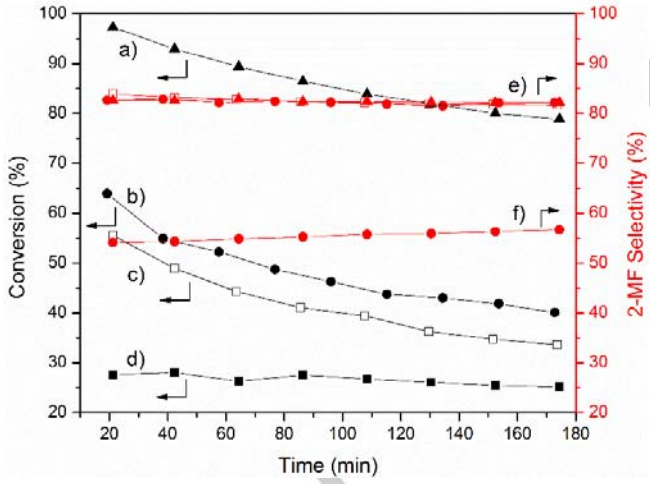

Figure 3: Time on stream data of FA conversion and 2-MF selectivity over various 3Co-xFe-yAl catalysts at W/F (g_{cat}*h*mol^{-1}) = 3.63, 180 °C, 1 atm, and FA conc = 0.0015 mmol/mL; Black lines represent conversion and red lines represent 2-methylfuran selectivity. a) 3Co-0.25Fe-0.75Al; b) 3Co-0.5Fe-0.5Al; c) 3Co-0.75Fe-0.25Al; d) 3Co-Al; e) 3Co-xFe-yAl; f) 3Co-Al.

Initial testing helped distinguish the effects of Fe addition into the Co-Al matrix. It is clear that the addition of Fe significantly enhances the activity of the catalysts, while also increasing the selectivity towards the desired product. In all samples that contained Fe, the selectivity towards 2-MF hovered around 83% while 2-MF selectivity for the 3Co-Al was between 53%-57%. The 3Co-Fe catalyst is not displayed due to its inactivity under the conditions used for these reactions. A wide variety of other products were obtained due to the many side reactions and series reactions that are possible (Table S1). Additional products include furan, 2-MTHF, 1-butanol (1-BOL), 2-pentanone (2-PONE), 1-pentanol, 2-pentanol, etc., the latter of which are a result of ring-saturation, decarbonylation, and ring-opening. Interestingly, some hydrocarbons were observed, such as propane and butane, which indicates minor hydrocracking pathways similar to what was previously observed over a Cu/Cr/Ni/Zn/Fe catalyst in the vapor phase hydrogenation of 2-MF.[30] At simila WHSV, the Co catalysts with lowest Fe addition displayed the highest activity, followed by 3Co-0.5Fe-0.5Al and 3Co-0.75Fe 0.25Al. To assess if even lower Fe loading might further elevate the catalytic activity, a catalytic test was performed on a lower Fe loaded catalyst (3Co-0.125Fe-0.875) which demonstrated an incrementa increase in conversion (99% after 40 min on stream) with nc variation in selectivity. This suggested that there may be ar optimum in regards to activity at lower Fe loadings, elevating activity above that of 3Co-0.25Fe-0.75Al. Since further characterizatior studies, such as XAS, at lower Fe loadings would have been difficul only the higher loaded catalysts were chosen for further studies.

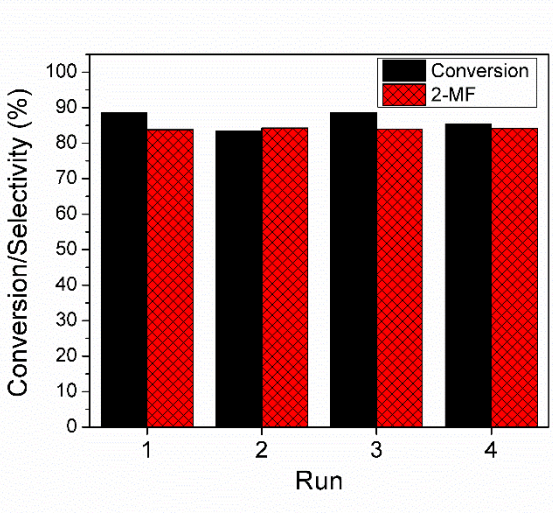

Figure 4: Recycle tests of 3 Co-0.25Fe-0.75Al displaying conversion and selectivity towards 2-MF at W/F (g_{cat}*h*mol^{-1}) = 3.63 with FA as a substrate. Data point taken at approximately 40 min on stream.

Time on stream data indicated deactivation of all the catalysts ove time; however, little to no change in the selectivity occurred. Pos reaction TGA (Figure S12) experiments displayed little to no carbor deposition, which may suggest that the major deactivatior mechanism was not blocking of sites from carbon deposits. Additionally, recycle tests were conducted on the 3Co-0.25Fe-0.75Al catalyst, which included a calcination step at 400 °C in air for 4 h followed by a reduction step outlined in the experimental section.

Each of the catalysts in the recycle test was run for approximately 150 min. The recycle tests demonstrated the catalysts regained their initial activity upon reuse over 3 recycles, as shown in Figure 4. This may indicate the mixed metal oxide matrix prepared through the co-precipitation method does not facilitate irreversible sintering after reduction and the mildly deactivated sample can be easily regenerated. A more likely deactivation mechanism could be through the oxidation of metallic sites, since 2-MF production creates H_2O, potentially causing surface oxidation similar to what Resasco et al. observed over Ni-Fe/SiO_2.[6] However, operando spectroscopic studies would need to be conducted to further verify the major deactivation mechanism.

Further investigations of the 3Co-0.25Fe-0.75Al catalyst were conducted as a function of the weight hourly space velocity, W/F. Figure 5 shows the conversion and selectivity of 2-methylfuran along with significant minor products while the temperature and pressure remained constant at 180 °C and 1 atm. The values were obtained at approximately 40 min on stream after the system reached a pseudo steady-state.

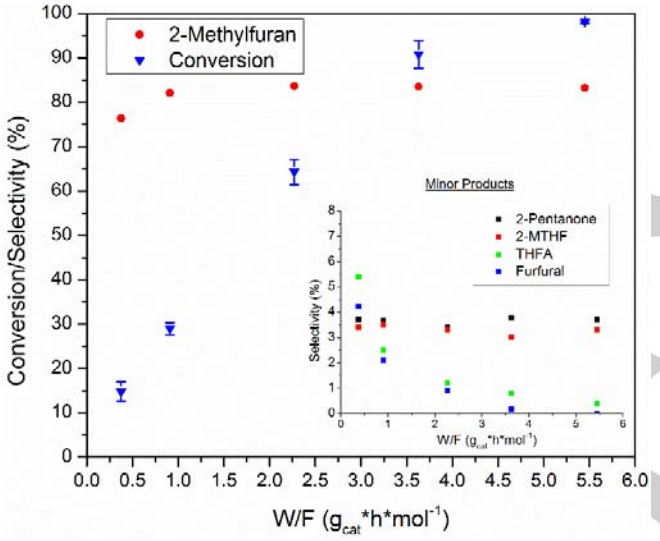

Figure 5: Varying W/F of the 3Co-0.25Fe-0.75Al catalyst at 180 °C and 1 atm with a FA flow rate varying between 5.5-12 mmol/h and H_2 flow rate varying between 60-130 mL/min while keeping the FA concentration at 0.0015 mmol/mL. Inset graph displays the selectivity of significant minor products over varying W/F. Values taken at approximately 40 min on stream.

As expected, conversion increases with an increase in residence time, but interestingly, at high W/F, there is noticeably little difference in the selectivity towards 2-MF (80-85%). On the contrary, when lower residence times were used there was an incremental decrease in 2-MF selectivity, and an increase in ring saturation products, THFA, and FUR. These results were reproducible yet unexpected since THFA and FUR are not intermediates to 2-MF. The observation is likely a result of differing surface coverages of various species, but more mechanistic studies and density functional theory calculations would need to be conducted to determine the root cause of ring-saturation propensity to THFA only at lower conversions.

Investigations into the reactivity of FUR over the Co-Fe-Al catalysts were conducted to verify reaction pathways and to determine if additional side products emerged. Various weight hourly space velocities were tested utilizing the 3Co-0.25Fe-0.75Al catalyst due its greater activity for FA conversion. As expected, the data for FUR conversion in Table 2 demonstrate an increase in conversion with an increase in catalysts loading, and an increase in 2-MF selectivity as the conversion increases. Similarly, the yield to FA seems to decrease linearly with the increase in 2-MF, confirming the series reaction of FUR to FA to 2-MF observed in prior literature.[9]

A combined selectivity towards 2-MF and FA of 75-79% was achieved at a variety of conversion levels. An important distinction between reactions between FA and FUR was the slight decrease in carbon balance when FUR was fed into the reactor, and significantly more unknown peaks were visible at high retention times, indicating more oligomer formation from FUR. Though the carbon balance closed within 91% for each FUR run, there was a clear indication of the increased propensity of FUR oligomerization with itself or other unidentifiable side products.[31,32] Deactivation was also observed during continuous flow similar to the deactivation with FA as the substrate. Ultimately, a yield of 60% towards 2-MF was achieved when feeding FUR, which is equivalent to or better than most prior literature using vapor phase reactions.[9,15,16,33] Though a very recently study of imbedded Cu in SiO_2 demonstrated higher yields towards 2-MF in the vapor phase when FUR was fed as the reactant the reactions were conducted mainly above 220 °C.[34,35]

Further characterization of these complex mixed metal oxides was carried out to better understand the electronic environment of the catalyst before reaction. X-ray photoelectron spectroscopy was utilized to probe the catalytic surface after reduction; however, due to pyrophoric nature of the reduced catalyst, a 1 h passivation step at room temperature in 1% O_2 was conducted prior to employing the characterization technique. As shown in Figure S5, there is a clear change in the Co species before and after reduction/passivation of the 3Co-0.25Fe-0.75Al sample. Prior to reaction, the spectrum mimics Co_3O_4 due to the lack of a $2p_{3/2}$ satellite peak and the peak maximum of $2p_{3/2}$ at approximately 780.5 eV.[26,36–38] The emergence of a shoulder after reduction at approximately at 778 eV and the presences of a satellite peak, indicates the reduction of Co_3O_4 to CoO and Co^0.[36] With regards to the Fe species, very little change is indicated before and after reduction/passivation, with the peak maximum around 712 eV. This maximum is located at higher eV than standard Fe oxides (FeO, Fe_3O_4, and Fe_2O_3), which may further support the strong interaction between Fe and Co, causing

Table 2: Reaction data of FUR over 3Co-0.25Fe-0.75Al at 180 °C at various W/F

W/F (g_{cat}*h*mol^{-1})	Conversion (%)	2-MF (%)	FA (%)	Furan (%)	1-BOL (%)	2-PONE (%)	Others
3.63	45.0	43.7	35.0	3.9	2.6	1.4	13.4
7.27	83.0	57.1	19.2	4.5	3.8	1.5	13.9
10.91	90.0	66.6	8.5	4.0	3.9	2.4	14.6

Values obtained at approximately 40 min on stream. 1-BOL: 1-butanol, 2-PONE: 2-pentanone, others include hydrocarbons, MTHF, THFA, 1,2-PD, 1-pentanol, and 2-pentanol.

the Fe spectra to shift as a consequence of the more electronegative Co oxide.[39] XPS suggests that the Fe oxide species hardly reduced or that the passivation had enough of an impact to bring it close to its original state after initial reduction.

To further probe the catalyst structure, *in situ* X-ray absorption spectroscopy was used to investigate the electronic environment of these materials before and after reduction without the need to passivate the catalyst. The same catalyst pretreatment conditions were implemented at ANL, and scans were taken at room temperature to reduce the effect of the Debye-Waller factor, a correction for thermal vibration effects.[40,41] After investigating the Co k-edge before reduction and matching each spectrum to standards, it was clear by X-ray absorption near-edge structure (XANES, Figure S6) and extended X-ray absorption fine structure (EXAFS) analysis that the major species was Co_3O_4, which matches XPS results (Figure S5). There was no indication of additional spinel structures formed including $CoFe_2O_4$ or $CoAl_2O_4$, though there may still be strong interactions between the various oxide species. Once the samples were reduced for an hour in H_2, a clear change in the

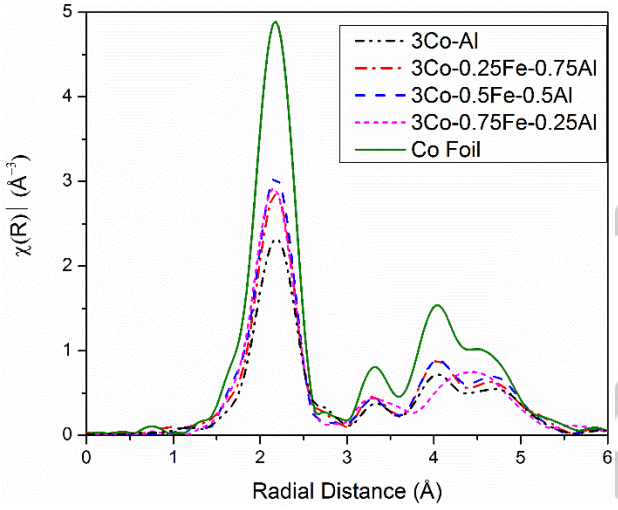

***Figure 6**: Fourier transformed EXAFS of Co k-edge post reduction at 500 ºC. Scans were taken at room temperature, and the k range displayed is 2.7-12 Å^{-1} with a k weight of k^2*

Co species was indicated by the major shift in the white line XANES of each catalyst and the emergence of a new peak in EXAFS analysis. Near edge analysis did indicate that the majority of the Co species were in a metallic state (Table S3). EXAFS analysis of the catalyst post reduction displayed one major feature at the 1st shell, which corresponds to Co-Co (Fe) scattering peak associated to a FCC structure, similar to that of Co foil and stable metallic Co.[42] Fitting of each catalyst using Co foil as a reference was conducted to determine the coordination number or Co-Co (Fe) species, since the magnitude of the peaks are significantly lower than the foil. The parameters of the fit are given in Table 3, and example fits are shown in Figure S10 and S11.

All of the R factors are <0.03, indicating good agreement with the experimental data and the curve fits. Upon fitting of each spectrum it became clear that there was no significant contribution of a Co-C scattering peak, indicating that the majority if not all the Co species were reduced to a metallic state. Additionally, even though there were Fe species most likely intercalated into the Co species, the Co Co(Fe) bond distance was within error of the metallic standard. This may be due to the high amount of Co in the sample as well as Co and Fe atomic radius being very similar. The most notable difference between the standard and the fitted catalysts after treatment was the clear reduction in coordination number of each o the samples tested, indicating the formation of particles and not a bulk-like and significantly aggregated metallic structure. Compared to the 3Co-Al catalyst, all of the 3Co-xFe-yAl catalysts had a mino increase in coordination number, which may be due to the reduction of Fe that becomes coordinated with Co or increased ease o reduction, supported by TPR, causing increased aggregation Further investigation of the Fe k-edge provided more evidence of a change in the electronic environment after reduction. The Fourie transformed EXAFS data are displayed in Figure 8, and they show a significant difference between each 3Co-xFe-yAl catalyst. After reduction, there was clear increase in the peak height of the 1st shell

Fitting of the Fe EXAFS spectra proved to be more complicated than for the Co region since the Co k-edge is approximately 600 eV after Fe k-edge. This limits the EXAFS range of Fe, causing fewe independent variables available for the fitting. Additionally, the complexity and potential inhomogeneity of each species in the sample results in an increase in constraints. XANES analysis of the Fe k-edge in Figure S9 indicates qualitatively that there may be a significant presence of FeO for a few samples, which may require a Fe-O scattering peak within the EXAFS fit. Additionally, fits withou the inclusion of Fe-O proved to be poor for the 3Co-0.25Fe-0.75A

Table 3: EXAFS results for the Analysis of Co k-edge post reduction[a]

Sample	Shell	CN	r (Å)	Δσ (10^{-3} Å^2)	ΔE$_0$ (eV)	R factor
Co foil[b]	Co-Co	12	2.50 ± 0.01	6.4 ± 0.4	7.8 ± 0.5	0.008
3Co-Al	Co-Co	5.7 ± 0.6	2.49 ± 0.01	6.5 ± 0.9	8.6 ± 1.1	0.015
3Co-0.25Fe-0.75Al	Co-Co(Fe)	6.9 ± 0.6	2.49 ± 0.01	6.5 ± 0.7	7.7 ± 0.8	0.007
3Co-0.5Fe-0.5Al	Co-Co(Fe)	7.8 ± 0.4	2.49 ± 0.01	6.9 ± 0.4	7.1 ± 0.5	0.003
3Co-0.75Fe-0.25Al	Co-Co(Fe)	7.1 ± 0.3	2.47 ± 0.01	6.5[c]	7.3 ± 1.0	0.013

[a]Fitting parameters: Fourier transform range, Δk, 2.7-12 Å^{-1} with weighting k^2. [b]Fourier transform range, Δk, 2.7-14 Å^{-1} with weighting k^2. Coordination number assigned from standard FCC Co^0 structure; S$_0^2$ (Co-Co) = 0.806 determined from Co foil fitting. [c]The Debye-Waller factor was fixed to the average to keep consistency with the other samples/model.

and 3Co-0.5Fe-0.5Al samples. Furthermore, in both 3Co-0.25Fe-0.75Al and 3Co-0.5Fe-0.5Al, the Fe-Fe(Co) peaks for metallic Fe were modelled as a FCC structure while for 3Co-0.75Fe-0.25Al the

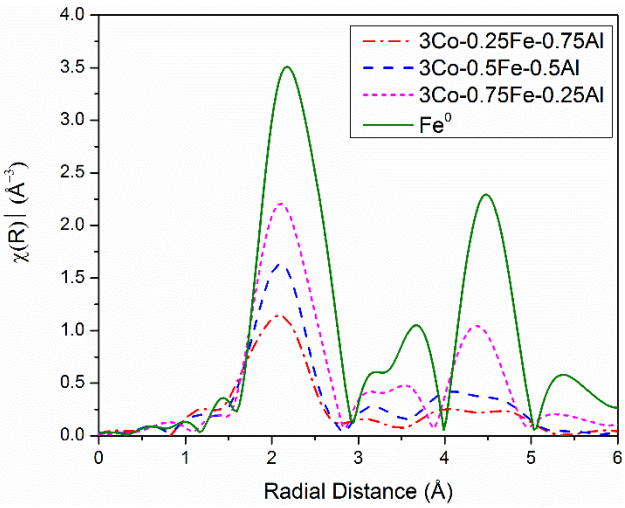

Figure 7: Fourier transformed EXAFS of Fe k-edge post reduction at 500 ºC. Scans were taken at room temperature, and the k range displayed is 2.7-10.5 $Å^{-1}$ at a k weight of k^2.

Fe-Fe(Co) peak was modelled after a BCC crystal structure, similar to that of Fe foil. This became necessary after attempts at fitting a BCC structure for all catalysts, and poor fits were obtained for the lower Fe loaded samples. Lastly, a qualitative evaluation of the 2nd shell (4-5 Å) shows the emergence of a major peak for 3Co-0.75Fe-0.25Al that mimics a BCC structure formation, while the other catalysts still mimic scattering peaks of the 2nd shell associated with FCC.[43] Therefore, for the two lower Fe loading catalysts, a model where Fe^0 atom is substituted into the FCC lattice of Co^0 and Fe-O scattering path was more consistent with the data collected. As a side note, Fe-Al bonds were neglected since there was no evidence of alloying of Al species, and there was only existence of an Al^{3+} oxide structure. Table 4 displays the best fit and the structural parameters associated with each.

Analysis of the Fe k-edge proved to have a more significant difference than the Co k-edge for each catalyst. Even though the majority of the Co species were in metallic form, the Fe species still maintained some Fe oxide species in the lower Fe loaded samples. Additionally, through various model tests, EXAFS suggested that the 0.25 and 0.5 Fe loaded samples contained Fe^0 species that were substituted into the lattice of the FCC Co^0. This supports the hypothesis of good dispersity of each species resulting from the starting LDH precursor, and may suggest the formation of a bimetallic particle upon reduction. As the Fe loading increases EXAFS analysis suggests a BCC structure similar to bulk metallic Fe begins to emerge.[44] In regards to the Fe-O scattering path fitted in the two samples, the bond distance was determined to be approximately 2.00 Å, which is lower than a standard Fe-O in an FeO structure, 2.17 Å.[45] However, for an Fe-O bond incorporated into an $FeAl_2O_4$ matrix the bond distance is approximately 1.95 Å which suggests that Al influences the Fe-O bond distance decreasing the overall average bond distance.[46]

Unlike the Co EXAFS analysis, there is a clear trend in which there was an increase in metal-metal coordination as the amount of Fe increased. This correlated well with TPR, which indicated that the higher Fe loading materials were easier to reduce overall. The increase in metal-metal coordination was indicative of aggregation which could result in larger particle sizes. This larger particle size and loss in metallic surface area supported the loss in activity per gram of catalyst for higher Fe loading materials, as shown in Figure 3. Additionally, at the higher Fe loading it may have be possible that the metallic Fe phases are beginning to separate from Co due to the formation of a BCC structure. Though reactivity studies showed there was no indication of a change in active sites since the selectivities do not vary, the loss in activity may be due to the loss in the amount of active sites due to metal aggregation. The highly dispersed Fe species for each catalyst may provide an electronic effect on the majority metallic Co species present in the catalysts,

Table 4: EXAFS results for the analysis of Fe k-edge post reduction[a]

Sample	Shell	CN	r (Å)	Δσ (10^{-3} $Å^2$)	ΔE_0 (eV)	R factor
Fe Foil[b]	Fe-Fe_{edge}	8	2.46 ± 0.01	5.0 ± 0.5	5.2 ± 1.3	0.004
	Fe-Fe_{center}	6	2.85 ± 0.01	7.5 ± 1.1	5.2 ± 1.3	
Fe(III)acac[c]	Fe-O	6	1.93 ± 0.01	10.3 ± 0.8	-0.5 ± 1.2	0.012
3Co-0.25Fe-0.75Al	Fe-O	2.1 ± 0.6	2.01 ± 0.02	9.5[e]	-5.9 ± 1.0	0.027
	Fe-Co(Fe)[d]	3.6 ± 0.3	2.49[f]	6.5[f]	-5.9 ± 1.0	
3Co-0.5Fe-0.5Al	Fe-O	1.4 ± 0.5	1.99 ± 0.03	9.9[e]	-3.6 ± 0.6	0.013
	Fe-Co(Fe)[d]	5.1 ± 0.3	2.49[f]	6.9[f]	-3.6 ± 0.6	
3Co-0.75Fe-0.25Al	Fe-Fe_{edge} (Co)	5.6 ± 0.7	2.44 ± 0.01	5.3 ± 0.1	-3.7 ± 2.7	0.006
	Fe-Fe_{center} (Co)	4.2 ± 0.5	2.82 ± 0.01	7.7 ± 0.2	-3.7 ± 2.7	

[a]Fitting parameters: Fourier transform range, Δk, 2.7-10.5 $Å^{-1}$ and R range, ΔR, of 1.2-3.0 Å with weighting k^2 unless stated otherwise. [b]Fourier transform range, Δk, 2.3-13 $Å^{-1}$ with weighting k^2; Coordination number assigned from standard BCC Fe^0 structure; S_0^2 (Fe-Fe) = 0.733 determined from Fe foil fitting. [c]Coordination number assigned from standard Fe(III) acetylacetonate structure; R range, ΔR, of 1.1-2.2 Å and S_0^2 (Fe-O) = 0.721 determined from fitting. [d]Modelled after Co^0 FCC structure where Fe^0 replaces Co^0 atoms. [e]Manually optimized Debye-Waller factor. [f]Constrained values to corresponding Co-Co from Co EXAFS fitting since the model is Fe^0 replacing Co^0 in the lattice.

which may lead to minimal change in selectivtiy over the different Fe/Al ratios. Lastly, the small amount of Fe oxide present in the samples with lower Fe loadings may facilitate the adsorption of the highly oxygenated compound allowing for an increase in activity per gram of catalyst, similar to what was observed with a partially reduced Fe species mixed in a Cu-Fe/SiO_2 catalyst.[11] Unfortunately, due to the complexity of these catalysts and the highly oxophilic nature after reduction (discussed above with XPS characterization) it proved difficult to measure the active site density on the catalyst post reduction, and thus TOFs are not reported.

Conclusion

Co based mixed metal oxides were derived from the calcination of LDH materials, yielding porous, thermally stable, non-precious metal catalysts for the hydrogenolysis of FA to 2-methylfuran, a promising biomass derived fuel additive. By utilizing the LDH synthesis method, a well-dispersed solid solution between each oxide domain was formed, which was supported by the weak/broad diffraction peaks in each XRD pattern. Additionally, the method allowed for the simple addition of other metal components such as Fe, which drastically impacted the electronic environment of the catalyst without significant deviations in physical properties (N_2 physisorption and XRD). An array of Co-Fe-Al catalysts with varying Co:Fe ratios were investigated in a vapor phase flow reactor, and prior to reaction the catalysts were reduced *in situ* in an H_2 atmosphere. Through XAS analysis, it was evident that the reduction parameters conducted allowed for the almost full reduction of Co_3O_4 for each catalyst, with varying degrees of reduction for the Fe species. As the loading of Fe increased, there was an increase in Fe reduction due to the ease of Fe oxide reduction over Al_2O_3, which may contribute to increased aggregation of metallic species and a loss in surface area. This was evident during reactivity studies, which showed that the activities for each Co-Fe-Al catalyst followed as such: 0.25Fe > 0.5Fe > 0.75Fe. Despite differences in activity among the Fe loaded samples, it was evident that the addition of Fe enhanced both the activity per gram and selectivity towards 2-MF compared to the 3Co-Al catalyst. Furthermore, the 3Co-0.25Fe-0.75Al catalyst exhibited high selectivities towards 2-MF over a range of conversions (75%-84%). The ability to recycle these catalysts was shown after calcining and re-reducing the catalysts. Through this study, it is evident that mixed metal oxides derived from LDH materials can yield multi-metal systems where there is good interaction between each component, which can produce selective catalysts for FA and FUR conversion. Further investigations on various additives into an LDH matrix may allow for additional tuning to reduce catalyst deactivation or enhance the yield to 2-MF even further.

Experimental Section

Materials and Chemicals

Furfural (99% purity, ACS Grade) and Furfuryl Alcohol (98% purity) were purchased from Sigma Aldrich, vacuum distilled, and then stored in inert atmosphere before use in reactions. $Co(NO_3)_2{\cdot}6H_2O$ (99% purity), Na_2CO_3 (99.5% purity), and ethylene glycol diethyl ether (98% purity) were purchased from Sigma Aldrich. $Fe(NO_3)_3{\cdot}9H_2O$, and $Al(NO_3)_3{\cdot}9H_2O$ were all purchased from Alfa Aesar (98%-102%). NaOH (97% purity) was purchased from EMD. Lastly, unless noted, all chemicals were used as is without any further purification.

Catalyst Synthesis

Co-Fe-Al mixed metal oxides with varying Co:Fe ratios of 12:1, 6:1, 4:1, 3:1, and no Fe addition (Co/(Fe+Al) always kept at 0.25) were prepared in the following manner, similar to prior LDH syntheses, with minor modifications.[26,47] A 0.6 M metal nitrate solution, Solution A, with corresponding metal cations ratios above, and a 1.0 M NaOH solution, Solution B, were created. A 0.3 M solution of Na_2CO_3, Solution C, was placed in a 3-neck, 1 L flask, and using a peristaltic pump Solution A and Solution B were added dropwise into Solution C at approximately 5 mL/min under vigorous stirring, at room temperature, with N_2 bubbling. The pH was maintained at 10 by adjusting Solution B. The pump was shut off once Solution A ran out, and the final solution was heated to 60 °C, and maintained under vigorous stirring and N_2 bubbling for 24 h. Once complete, the final solution was filtered and washed until the filtered solution had a pH of ~7 (about 1.5 L of DI water was used) to obtain the LDH precipitant. The recovered solid was dried in an oven at 105°C overnight. To create the mixed metal oxide, the dried LDH material was calcined at 400°C with 50 mL/min flow of air with a ramp rate of 10°C/min, being held at 400°C for 4 hours.

Reaction Studies

Vapor phase reactions were performed in a ¼" tubular stainless steel reactor located inside a furnace. The catalyst was pelletized (>270 mesh), diluted with SiC (200-400 mesh), and loaded into the reactor between layers of SiC (46 mesh) and quartz wool. The catalysts were reduced *in situ* under 60 mL/min H_2 (Airgas, UHP) to 500˚C with a ramp rate of 5°C/min, then subsequently held for one hour. Once the reduction was completed, the bed was cooled under H_2 to reaction temperature, which was typically conducted at 180 °C. Unless stated otherwise, reactions were conducted in a flow of 60 mL/min of H_2, while FA was pumped into the vaporization zone at a rate of 5.5 mmol/h (with ~4 mol% ethylene glycol diethyl ether as internal standard). The FA flow met heated H_2 in the vaporization zone, which was heated to approximately 180 °C. The vapor flowed through the catalyst bed, and then it flowed into an online Agilent 7890A GC through lines heated to approximately 185°C to mitigate reactant and product condensation. Selectivity and conversion were determined by the internal standard method and carbon balances were within 95% typically due to small amounts of unknown products, unless stated otherwise. After the reaction or reduction was completed, the catalyst was passivated for one hour at room temperature under 1% O_2/N_2 (Airgas), separated form SiC, and stored under argon for further characterization studies.

Characterization Techniques

Nitrogen physisorption was performed in a Micromeritics Tristar II at -196°C after the samples were pretreated at 200°C under vacuum for 12 h. Chemisorption and TPR experiments were conducted in a Micromeritics AutoChem II 2920. For each experiment, approximately 50 mg of sample was placed on top of a small bed of quartz wool in a quartz U-tube. In regards to the TPR experiment, the mixed metal oxide was pretreated in 20 mL/min of He (Airgas, UHP) at 200°C for 2 h to remove pre-adsorbed species. The sample was then cooled to 50°C and 20 mL/min of 10% H_2 (balance Ar) was passed through the sample. The furnace was heated to 800°C at 5°C/min while under the flow of 10% H_2/Ar. The outlet gas passed through a liquid acetone/nitrogen trap, and then was passed through a thermal conductivity detector (TCD). Elemental analysis for each catalyst was conducted at the Georgia Tech Renewable Bioproducts Institute on an inductively coupled plasma optical emission spectroscopy (ICP-OES) instrument, a PerkinElmer OPTIMA 7300 DV, after dissolving the metal oxides in dilute H_2SO_4 solution.

Powder X-Ray diffraction patterns were collected using a Philips X-per diffractometer using Cu Kα radiation. X-Ray Photoemission Spectroscopy (XPS) analysis was performed using a Thermo K-Alpha spectrometer employing a monochromatic Al Kα. The pressures inside the analytical chamber was approximately $1x10^{-7}$Torr. The binding energies (BE) of all elements were tuned to the Ag 3d peak (368.2 eV) with an uncertainty of ± 0.2 eV.

In situ X-ray absorbtion spectroscopy (XANES and EXAFS) were conducted at the Advanced Photon Source (APS), Argonne National Lab (ANL) at beamline 12-BM. The data were obtained in transmission mode at the Fe K-edge (7112 eV) in the range of 6910-7910 eV, and the Co K-edge (7712 eV) in the range of 7510-8712 eV, both with a spot size of 0.5 mm x 1.2 mm. To perform the *in situ* reduction XAS, the catalyst sample was diluted and ground with boron nitride (5:1 BN: catalyst), and then ~8 mg of the

mixture was loaded and pressed into a "six shooter" holder (multiple samples could be pressed into the holder). This holder was then placed into a quartz tube with Kapton windows at each end to allow X-rays to pass through, and a gas line was attached to the tube. A scan was collected prior to reduction at room temperature. Next, the catalyst was heated to 500°C at 5°C/min and held for 1 h, all while under a 60 mL/min flow of pure H_2. After the reduction was complete, the sample was cooled down in H_2, and a final scan was collected at room temperature. Various standards were used to verify the species present in the catalyst sample. The XAS data were processed and analyzed with Athena software including background removal, edge-step normalization, and Fourier transform. Artemis software was utilized to fit the Fourier transformed EXAFS data with a model. Co-Co, Fe-Fe, Fe-O reference parameters were calculated using Co foil (FCC), Fe foil (BCC), and Fe(III) acetylacetonate as standards. Multiple scattering paths through crystallographic data including, Co-Co[48], Fe-Fe[49], Fe-O-Fe[45], Fe-O-Al[46], and Fe-Al[50], were calculated using FEFF8.[51] Due to the complexity of the matrix, various constraints were added on the Debye-Waller factor and bond distances for some of the catalysts, similar to previous bimetallic systems.[52,53]

Acknowledgements

This work was supported as part of the Catalysis Center for Energy Innovation, an Energy Frontier Research Center funded by the U.S. Department of Energy, Office of Science under grant DE-SC0001004. We would also like to thank Dr. Faisal Alamgir for a discussion on EXAFS fitting.

XAS studies were conducted using resources at the Advanced Photon Source, a U.S. Department of Energy (DOE) Office of Science User Facility operated for the DOE Office of Science by Argonne National Laboratory under Contract No. DE-AC02-06CH11357.

Keywords: biomass • furanics • hydrogenation • cobalt-iron catalysts • XAS

[1] P. Gallezot, *Chem. Soc. Rev.* **2012**, *41*, 1538–1558.
[2] D. M. Alonso, J. Q. Bond, J. A. Dumesic, *Green Chem.* **2010**, *12*, 1493–1513.
[3] X. Li, P. Jia, T. Wang, *ACS Catal.* **2016**, *6*, 7621–7640.
[4] Y. Román-Leshkov, C. J. Barrett, Z. Y. Liu, J. A. Dumesic, *Nature* **2007**, *447*, 982–985.
[5] L. W. Burnett, I. B. Johns, R. F. Holdren, R. M. Hixon, *Ind. Eng. Chem.* **1948**, *40*, 502–505.
[6] S. Sitthisa, D. E. Resasco, *Catal. Letters* **2011**, *141*, 784–791.
[7] Y. Nakagawa, H. Nakazawa, H. Watanabe, K. Tomishige, *ChemCatChem* **2012**, *4*, 1791–1797.
[8] D. M. Alonso, S. G. Wettstein, J. A. Dumesic, *Chem. Soc. Rev.* **2012**, *41*, 8075–8098.
[9] S. Sitthisa, W. An, D. E. Resasco, *J. Catal.* **2011**, *284*, 90–101.
[10] W. Yu, K. Xiong, N. Ji, M. D. Porosoff, J. G. Chen, *J. Catal.* **2014**, *317*, 253–262.
[11] H. Sheng, R. F. Lobo, *ChemCatChem* **2016**, *8*, 3402–3408.
[12] M. Manikandan, A. K. Venugopal, A. S. Nagpure, S. Chilukuri, T. Raja, *RSC Adv.* **2016**, *6*, 3888–3898.
[13] D. Shi, J. M. Vohs, *ACS Catal.* **2015**, *5*, 2177–2183.
[14] H.-Y. Zheng, Y.-L. Zhu, Z.-Q. Bai, L. Huang, H.-W. Xiang, Y.-W. Li, *Green Chem.* **2006**, *8*, 107–109.
[15] H.-Y. Zheng, Y.-L. Zhu, B.-T. Teng, Z.-Q. Bai, C.-H. Zhang, H.-W. Xiang, Y.-W. Li, *J. Mol. Catal. A Chem.* **2006**, *246*, 18–23.
[16] W.-S. Lee, Z. Wang, W. Zheng, D. G. Vlachos, A. Bhan, *Catal. Sci. Technol.* **2014**, *4*, 2340–2352.
[17] P. Yang, Q. Cui, Y. Zu, X. Liu, G. Lu, Y. Wang, *Catal. Commun.* **2015**, *66*, 55–59.
[18] Y. Zu, P. Yang, J. Wang, X. Liu, J. Ren, G. Lu, Y. Wang, *Appl. Catal. B Environ.* **2014**, *146*, 244–248.
[19] Y.-B. Huang, M.-Y. Chen, L. Yan, Q.-X. Guo, Y. Fu, *ChemSusChem* **2014**, *7*, 1068–1072.
[20] G. Wang, J. Hilgert, F. H. Richter, F. Wang, H. Bongard, B. Spliethoff, C. Weidenthaler, F. Schüth, *Nat. Mater.* **2014**, *13*, 293–300.
[21] Y. Zhu, X. Kong, H. Zheng, G. Ding, Y. Zhu, Y.-W. Li, *Catal. Sci. Technol.* **2015**, *5*, 4208–4217.
[22] P. Panagiotopoulou, D. G. Vlachos, *Appl. Catal. A Gen.* **2014**, *480*, 17–24.
[23] S. Srivastava, G. C. Jadeja, J. Parikh, *RSC Adv.* **2016**, *6*, 1649–1658.
[24] S. Iqbal, X. Liu, O. F. Aldosari, P. J. Miedziak, J. K. Edwards, G. L. Brett, A. Akram, G. M. King, T. E. Davies, D. J. Morgan, et al., *Catal. Sci. Technol.* **2014**, *4*, 2280–2286.
[25] B. Chen, F. Li, Z. Huang, G. Yuan, *Appl. Catal. B Environ.* **2017**, *200*, 192–199.
[26] T. P. Sulmonetti, S. H. Pang, M. T. Claure, S. Lee, D. A. Cullen, P. K. Agrawal, C. W. Jones, *Appl. Catal. A Gen.* **2016**, *517*, 187–195.
[27] S. Nishimura, A. Takagaki, K. Ebitani, *Green Chem.* **2013**, *15* 2026–2042.
[28] A. A. Khassin, T. M. Yurieva, G. N. Kustova, I. S. Itenberg, M. P. Demeshkina, T. a. Krieger, L. M. Plyasova, G. K. Chermashentseva, V. N. Parmon, *J. Mol. Catal. A Chem.* **2001**, *168*, 193–207.
[29] J. Sun, A. M. Karim, H. Zhang, L. Kovarik, X. S. Li, A. J. Hensley, J. S. McEwen, Y. Wang, *J. Catal.* **2013**, *306*, 47–57.
[30] P. Biswas, J.-H. Lin, J. Kang, V. V. Guliants, *Appl. Catal. A Gen.* **2014**, *475*, 379–385.
[31] Y. Nakagawa, M. Tamura, K. Tomishige, *ACS Catal.* **2013**, *3*, 2655–2668.
[32] K. Yan, G. Wu, T. Lafleur, C. Jarvis, *Renew. Sustain. Energy Rev.* **2014**, *38*, 663–676.
[33] J. Luo, M. Monai, H. Yun, L. Arroyo-Ramírez, C. Wang, C. B. Murray, P. Fornasiero, R. J. Gorte, *Catal. Letters* **2016**, *146*, 711–717.
[34] F. Dong, Y. Zhu, H. Zheng, Y. Zhu, X. Li, Y. Li, *J. Mol. Catal. A Chem.* **2015**, *398*, 140–148.
[35] F. Dong, G. Ding, H. Zheng, X. Xiang, L. Chen, Y. Zhu, Y. Li, *Catal. Sci. Technol.* **2016**, *6*, 767–779.
[36] M. C. Biesinger, B. P. Payne, A. P. Grosvenor, L. W. M. Lau, A. R. Gerson, R. S. C. Smart, *Appl. Surf. Sci.* **2011**, *257*, 2717–2730.
[37] A. A. Khassin, T. M. Yurieva, V. V. Kaichev, V. I. Bukhtiyarov, A. A. Budneva, E. a. Paukshtis, V. N. Parmon, *J. Mol. Catal. A Chem.* **2001**, *175*, 189–204.
[38] Q. Yang, H. Choi, S. R. Al-Abed, D. D. Dionysiou, *Appl. Catal. B Environ.* **2009**, *88*, 462–469.
[39] M. J. Guittet, J. P. Crocombette, M. Gautier-Soyer, *Phys. Rev. B* **2001**, *63*, 125117.
[40] M. M. Günter, T. Ressler, R. E. Jentoft, B. Bems, *J. Catal.* **2001**, *203*, 133–149.
[41] V. M. Gonzalez-delacruz, R. Pere, F. Ternero, J. P. Holgado, A. Caballero, *J. Phys. Chem. C* **2012**, *116*, 2919–2926.
[42] N. E. Tsakoumis, A. Voronov, M. Ronning, W. Van Beek, O. Borg, E. Rytter, A. Holmen, *J. Catal.* **2012**, *291*, 138–148.
[43] Y. Sekine, Y. Nakazawa, K. Oyama, T. Shimizu, S. Ogo, *Appl. Catal. A Gen.* **2014**, *472*, 113–122.
[44] Y. Hong, H. Zhang, J. Sun, K. M. Ayman, A. J. R. Hensley, M. Gu, M. H. Engelhard, J.-S. McEwen, Y. Wang, *ACS Catal.* **2014**, *4*, 3335–3345.

[45] E. R. Jette, F. Foote, *J. Chem. Phys.* **1933**, *1*, 29–36.
[46] R. J. Hill, *Am. Mineral.* **1984**, *69*, 937–942.
[47] M. Taborga Claure, S.-H. Chai, S. Dai, K. A. Unocic, F. M. Alamgir, P. K. Agrawal, C. W. Jones, *J. Catal.* **2015**, *324*, 88–97.
[48] R. W. G. Wyckoff, *Crystal Structures*, Interscience Publishers, New York, **1963**.
[49] P. M. Woodward, E. Suard, P. Karen, *J. Am. Chem. Soc.* **2003**, *125*, 8889–8899.
[50] N. Ridley, *J. Insitute Met.* **1966**, *94*, 255–258.
[51] S. Calvin, E. Carpenter, B. Ravel, V. Harris, S. Morrison, *Phys. Rev. B* **2002**, *66*, 224405.
[52] J. Batista, A. Pintar, J. P. Gomilsek, A. Kodre, F. Bornette, *Appl. Catal. A Gen.* **2001**, *217*, 55–68.
[53] A. F. Lee, C. J. Baddeley, C. Hardacre, R. M. Ormerod, R. M. Lambert, G. Schmid, H. West, *J. Phys. Chem.* **1995**, *99*, 6096–6102.

10.1002/cctc.201700228

WILEY-VCH

FULL PAPER

Co-Fe-Al oxides derived from layered double hydroxides can be reduced to form a catalytically active material for hydrogenolysis of furanics to 2-methylfuran

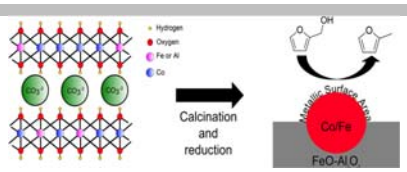

Taylor P. Sulmonetti,[a] Bo Hu,[a] Zachary Ifkovits,[a] Sungsik Lee,[b] Pradeep K. Agrawal[a] and Christopher W. Jones[a*]

Page No. – Page No.

Vapor Phase Hydrogenolysis of Furanics Utilizing Reduced Cobalt Mixed Metal Oxide Catalysts